# Variation Propagation Analysis on Compliant Assemblies Considering Contact Interaction

**Kang Xie**
**Lee Wells**
**Jaime A. Camelio**
**Byeng D. Youn**

Department of Mechanical Engineering–Engineering Mechanics, Michigan Technological University, Houghton, MI 49931

*Dimensional variation is inherent to any manufacturing process. In order to minimize its impact on assembly products it is important to understand how the variation propagates through the assembly process. Unfortunately, manufacturing processes are complex and in many cases highly nonlinear. Traditionally, assembly process modeling has been approached as a linear process. However, many assemblies undergo highly complex nonlinear physical processes, such as compliant deformation, contact interaction, and welding thermal deformation. This paper presents a new variation propagation methodology considering the compliant contact effect, which will be analyzed through nonlinear frictional contact analysis. Its variation prediction will be accurately and efficiently conducted using an enhanced dimension reduction method. A case study is presented to show the applicability of the proposed methodology.* [DOI: 10.1115/1.2752829]

## 1 Introduction

Dimensional variation is inherent to any manufacturing process. Therefore, it is important to understand how it propagates through a manufacturing process. Fast and accurate evaluation models of process variation are critical in determining the final dimensional variation of a product and in selecting robust product/process design. Unfortunately, manufacturing processes are complex and in many cases highly nonlinear. In general, the lack of efficient nonlinear modeling tools has limited the analysis of processes to simplified linear models.

One commonly used nonlinear manufacturing process is the assembly of compliant components. Compliant assembly is defined as the process of joining flexible or nonrigid parts. Many products, including automobiles, aircraft, furniture, and home appliances, are constructed primarily from compliant parts. In many of these products, the number of parts can be very large, such as the several hundred compliant parts that form a typical auto body assembly. Since parts and fixtures inherently have geometrical variation, understanding how these variations propagate through the system is of significant interest to the design and control of such systems. Two approaches have been widely adopted to model assembly processes: rigid body analysis [1,2] and compliant analysis [3–6]. However, all these methodologies are based on linearized models. In contrast, Cai et al. [7] introduced the nonlinear contact effect on the assembly of compliant parts. They used a second-order Taylor expansion (TSE) method to estimate the nonlinear effects. However, TSE methods are inefficient and inaccurate unless the assembly process response is close to being linear.

Variation propagation analysis is defined as a mechanism by which input uncertainty is propagated to output uncertainty through a system (or process). The system may consist of subsystems or subprocesses. Input uncertainty includes any type of parameters or variables that are uncertain, as shown in Table 1. Although uncertainty propagation has been extensively investigated in many engineering fields, uncertainty propagation is still regarded as a state-of the-art task, mainly due to its expensiveness and inaccuracy for complex systems.

Accordingly, many different methods have been developed for uncertainty propagation analysis. These methods can be categorized into three approaches: sampling techniques, expansion techniques, and advanced first-order second moment (AFOSM).

The most common sampling techniques are Monte Carlo simulation (MCS) and design of experiments (DOE). In general, these methods are quite comprehensive and easy to use but may be too expensive to achieve good accuracy. Simulation methods [3] can be expensive for predicting high reliability, whereas DOE [8] can be costly for high dimensional problems, a so-called curse of dimensionality. Therefore, sampling techniques are often used for verification or benchmarking studies.

There exist three types of expansion methods: Taylor series expansion, perturbation, and Neumann expansion. The Taylor series expansion method yields inaccurate estimates for a nonlinear system. Hence, its application has been restricted to linear or mildly nonlinear systems. In addition to such difficulty, it requires a second-order sensitivity analysis for uncertainty control, which is expensive and complicated [9]. In the perturbation method, the solution is approximately represented in a perturbed form. Thus, it can be applied to diverse systems represented by differential, integral, and algebraic equations. Its primary disadvantages are the lack of applicability to experiments and computational expensiveness when the dimension of the system is large [10]. Similarly, the main limitation of the Neumann expansion method is the requirement that the perturbation terms must be small. Further, this method is in general difficult to apply in conjunction with modeling complex nonlinear systems, as the model equations are often mathematically intractable [11]. It is quite interesting that the common drawback of expansion methods is inaccuracy of uncertainty characterization for nonlinear systems.

Depending on the order of system approximation, uncertainty propagation can be analyzed using AFOSM, such as first-order reliability method (FORM) and using second-order reliability method (SORM). These methods accurately predict a tail approximation of the probability distribution for a system but, respectively, require first-order and second-order derivatives for system performances with respect to input uncertainties [12]. Thus, the application of AFOSM is limited to relatively simple engineering problems.

Current assembly models for predicting geometrical variation propagation are limited to linear analysis. However, real assembly processes are more complex and heavily subject to uncertainties of system parameters. In order to extend the capabilities of current models, it is necessary to create new methods that predict geo-

Contributed by the Manufacturing Engineering Division of ASME for publication in the Journal of Manufacturing Science and Engineering. Manuscript received August 3, 2006; final manuscript received May 17, 2007. Review conducted by Shivakumar Raman.

  

**Table 1 Sources of uncertainty**

| Source | Uncertainty type | Examples |
|---|---|---|
| Product | Shape | Circularity |
| | Size | Length; thickness |
| | Configuration | Angles |
| | Material | Young's modulus |
| Process | Geometrical | Fixtures position; Welding gun location |
| | Process parameters | Pressure; sequence Welding temperatures; Current welding speed; Welding direction |

metrical variation propagation by taking into account the nonlinear effects due to the contact between the components and tools in the physical assembly process.

This paper presents a new methodology to predict the effect on assembly dimensions due to variation on geometrical dimensions on the assembly components. The methodology considers the assembly interaction due to the physical contact between the components and tools (clamps and welding guns). These interactions produce additional deformations in the components during and after the assembly process. In addition, due to the limitation of traditional uncertainty propagation methods, a new methodology for uncertainty propagation in nonlinear assembly systems is presented. The methodology is based on finite element calculations and an enhanced dimension reduction method [13,14].

The paper is organized as follows. Section 2 reviews the traditional rigid and compliant assembly methodologies. Section 3 presents the new methodology to predict assembly variation propagation in nonlinear contact assemblies. The enhanced dimension reduction (eDR) method is presented in Sec. 4. The eDR method allows predicting the output distribution for the assembly based on given distribution of the input parameters. In Sec. 5, a case study of a hood bracket assembly is discussed. The case study shows the application of the new methodology. Finally, Sec. 6 draws conclusions.

## 2 Traditional Sheet Metal Assembly Modeling

Several models have been proposed to predict variation propagation on assembly processes. Initial approaches have focused on rigid part assembly using either the root sum squares (RSS) method or MCS. A detailed review and discussion can be found in Ref. [15]. Recently, multilevel variation propagation models have also been developed. Mantripragada and Whitney [2] proposed a state transition model to predict the variation propagation in multistage assembly systems. Ding et al. [1] presented a state space model for dimensional control in sheet metal assembly assuming rigid parts. For compliant assembly, Liu and Hu [3] proposed a compliant assembly model to analyze the effect of deformation and springback on assembly variation by applying linear mechanics and statistics. Using finite element methods (FEMs), they constructed a sensitivity matrix to establish a linear relationship between the incoming part deviation and the output assembly deviation. Camelio et al. [4] extended this approach to multistation systems using a state space representation.

Assembly variation is estimated as a function of the components' geometry, process layout, and the contribution of various sources of variation. Three main sources of variation have been identified in sheet metal assembly: component variation, fixture variation, and joining method induced variation. The term part variation is defined in a general sense, including the mean deviation, $\mu$, and the variance of the deviation, $\sigma^2$, on parameters that describe the geometry of the component. Deviation is defined as the difference between the actual part dimension and the nominal dimension. Part deviation can be denoted as a vector $\mathbf{V} \in \mathbf{R}^{n\times 1}$, in which the elements correspond to deviations at each parameter. Traditional assembly modeling approaches define part deviation as point based considering only key control characteristics.

Liu and Hu [3] presented the method of influence coefficients (MIC) to predict the impact of the part deviation, $\mathbf{X}$, on the assembly deviation, $\mathbf{Y}$. Finite element methods and the MIC are used to obtain the sensitivity matrix, $S$, for a sheet metal assembly. The elements of the sensitivity matrix, $s_{ij}$, measure the sensitivity of the assembly at node $i$ to the incoming part deviation at node $j$. This approach considers a linear relationship between the incoming parts deviation and the final assembly deviation. Therefore, the assembly deviation, $\mathbf{Y}$, can be calculated using Eq. (1). By definition $\mathbf{Y}$ is the assembly deviation vector, where the column elements represent the assembly deviation at the key measurement points. $\mathbf{X}$ is the component deviation vector, where the elements represent the component deviation at the welding nodes

$$Y = \begin{bmatrix} y_{a_1} \\ y_{a_2} \\ \vdots \\ y_{a_m} \end{bmatrix} = \sum_{j=1}^{n} \begin{bmatrix} s_{1j} \\ s_{2j} \\ \vdots \\ s_{mj} \end{bmatrix} \cdot x_j = \begin{bmatrix} s_{11} & s_{12} & \dots & s_{1n} \\ s_{21} & s_{22} & \dots & s_{2n} \\ \vdots & \vdots & \vdots & \vdots \\ s_{m1} & s_{m2} & \dots & s_{mn} \end{bmatrix} \cdot \begin{bmatrix} x_1 \\ x_2 \\ \vdots \\ x_n \end{bmatrix} \tag{1}$$

$$\text{or} \quad \mathbf{Y} = \mathbf{S} \cdot \mathbf{X}.$$

The station level model presented in Eq. (1) describes the assembly variation behavior at a single station. However, sheet metal assembly processes are typically multilevel hierarchical manufacturing processes, where parts are joined together at different sequential or parallel stations. Dimensional variation will propagate from station to station based on incoming parts variation, fixture variation, and the joining process variation. The propagation effect of the dimensional variation can be modeled as a linear time discrete system, where the variable time, $k$, represents the station location (Eq. (2)); $\mathbf{A}$ is the state matrix; $\mathbf{X}$ is the state vector; $\mathbf{B}$ is the input matrix; $\mathbf{U}$ is the input vector; $\mathbf{W}$ is a perturbation vector; $\mathbf{Y}$ is the measurement/observation vector; $\mathbf{C}$ is the observation matrix; and $\mathbf{V}$ is a measurement system noise vector. Camelio et al. [4] developed a methodology to analyze the propagation of variation in compliant multistation assembly systems using a state space representation

$$\mathbf{X}(k) = \mathbf{A}(k) \cdot \mathbf{X}(k-1) + \mathbf{B}(k) \cdot \mathbf{U}(k) + \mathbf{V}(k)$$

$$\mathbf{Y}(k) = \mathbf{C}(k) \cdot \mathbf{X}(k) + \mathbf{V}(k) \tag{2}$$

Although the MICs, presented by Liu and Hu [3] and widely used on assembly variation simulation, can precisely and efficiently predict the assembly distribution based on the linear mechanics, it cannot be directly used for problems that behave in the nonlinear domain. One of the limitations of the MIC is that the assembly deformation is considered linear and no consideration to part interference is included. Therefore, the parts are allowed to penetrate each other when the come in contact during the assembly process. In addition, the MIC approach constructs the sensitivity matrix evaluation using the response of a nominal assembly under external displacements for each individual component and the assembly. An equivalent force for each source of variation is generated by exerting the corresponding deviation of the component departing from a nominal position. The forces and displacements are estimated using a finite element model. Then, the clamping effect is simulated by applying the equivalent force in the opposite direction to cause the component to recover it's nominal position. This approach differs significantly from the real assembly process, limiting its capacity to represent the process under nonlinear conditions. As it was mentioned earlier, nonlinear behavior on assembly systems can be common under the contact interaction between parts and due to welding distortion effects.

Based on these limitations, a new methodology to represent the assembly process is needed. Considering the actual capabilities of commercially available finite element packages, a good method will be a model that can represent the assembly process as close to reality as possible. The proposed new approach is able to better simulate the real assembly and allows system parameterization. The system parameterization is a powerful tool to characterize the response of the assembly for different sources of variation. Combining the finite element analysis (FEA) tool with the eDR method, the new methodology can efficiently and precisely handle nonlinear contact problems.

## 3 Modeling Assembly Variation Including Contact Considerations

Traditionally, an assembly process of sheet metal parts considers six steps: (1) the parts are located in the assembly station, a 3-2-1 locating fixture is used; (2) additional locators or clamps are closed to nominal, deforming the sheet metal part if the part is non-nominal; (3) the welding gun(s) is closed to nominal, producing additional deformations; (4) the parts are joined together using, in general, resistance spot welding; (5) the welding gun and clamps are released; and (6) the assembly springbacks. In order to precisely represent the assembly process, a similar process is simulated in finite elements using ABAQUS.

Considering the six steps in the assembly process, a new methodology based on finite elements was developed to predict components and tooling variation propagation in an assembly process. The two objectives of the new methodology are: (1) to represent the assembly process as close to reality as possible using finite elements; and (2) to incorporate the effect of the physical contact between the components and tools in the assembly. Two types of contact are considered: the tool/part interactions and the part/part interactions. The new methodology consists of the following four steps that represent the assembly process of compliant sheet metal parts:

1. The parts are located in the station. This is equivalent to constructing the finite element model. The compliant sheet metal parts are modeled as shell elements. The locators are simulated as single point displacement constraints. In addition, to enhance the capability of the model to handle the interaction between parts and tools, contact pair elements are defined. The contact areas include both the contact between components or parts and the contact between the tools and the components. The parts are modeled including any deviation from its nominal shape. In order to model uncertainty in some dimensions, the model is parameterized. Therefore, the components geometry and mesh can be modified by a small set of parameters.
2. The clamps are closed, deforming the individual components to their nominal position. Each clamp is modeled as a rigid body. In general, the stiffness of the clamps is much larger than the stiffness of the individual components. Therefore, this is a reasonable assumption. At this step, the clamp is moved towards the part, and the part is deformed due to the contact between the clamp and the part.
3. The welding guns are closed and the parts are joined together. The welding process is simulated in three substeps. First, the contact elements in each component corresponding to the welding area are assigned as bonded. Bonding is a property available for the contact pairs to determine the behavior of elements that come in contact. Second, an additional type of element is introduced. The welding nugget is represented by connector elements. These elements constrain the nodes in different parts to share the same degree of freedom (DOF). Finally, an additional finite element tool, microgap adjusting, is used to ensure that the welding area between parts is completely in contact.
4. The parts are released. At this state, the welding gun tools and additional locators and clamps are removed; then, the assembly geometry changes due to the springback effect.

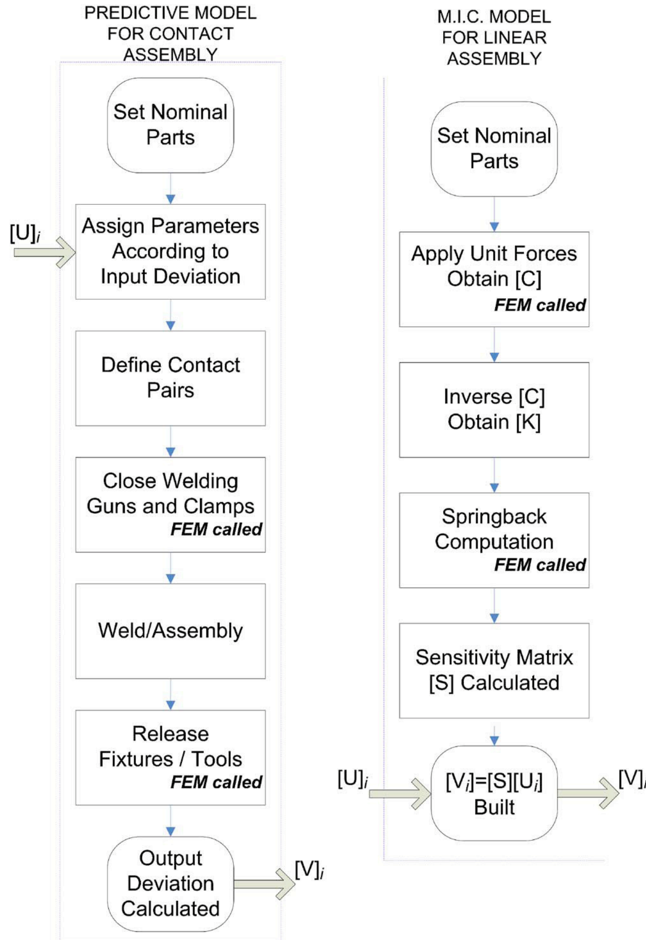


**Fig. 1 Predictive contact assembly and method of influence coefficients**

One of the main limitations of modeling contact elements is convergence of the finite element model. The proposed methodology has shown reliable results avoiding convergence issues. Several measures were taken to improve the convergence of the contact model. Some of the measures that improve the performance of the simulation included in the methodology are: (1) a fine mesh and fillets near the contact areas are used to avoid single node penetration; (2) connector elements representing the weld nugget are used to ensure sufficient constraint between welded parts; and (3) microgap adjusting is used to overcome the microgap and separation errors between the parts caused by the calculation errors in the finite element.

The proposed simulation process differs from the MIC presented by Liu and Hu [3] because it simulates the assembly process as a complete set of sequential operations without incorporating the use of equivalent forces or displacements to determine the final springback. Figure 1 shows the steps of each methodology. The main limitation of the new approach is that it requires a complete simulation to evaluate the final springback of the assembly for each set of input deviations. Due to the nonlinear response of the contact behavior, an expensive Monte Carlo simulation is required to completely describe the final distribution of the output dimensions considering some variability in the input parameters. To overcome this limitation, an efficient method to predict the variation propagation in nonlinear contact assembly processes is presented in Sec. 4

## 4 Enhanced Dimensional Reduction (DR) Method

**4.1 Dimension-Reduction (DR) Method.** In general, a probability density function (PDF) can be built using statistical moments (e.g., mean and standard deviation for normal distribution, and three parameters for Weibull distribution). First, statistical moments of a certain system response can be calculated as

$$\mathcal{E}\{Y^m(\mathbf{X})\} = \int_{-\infty}^{+\infty} \cdots \int_{-\infty}^{+\infty} Y^m(\mathbf{x}) \cdot f_{\mathbf{X}}(\mathbf{x}) \cdot d\mathbf{x} \tag{3}$$

Then, the corresponding PDF will be constructed based on statistical moments. Multidimensional integration is a major challenge in calculating statistical moments of system inputs. To resolve this difficulty, the dimension reduction (DR) method uses additive decomposition [13,16], which converts a multidimensional integration in Eq. (3) into multiple one-dimensional integrations. The additively decomposed function is defined as

$$\begin{aligned} Y(X_1, \ldots, X_N) \cong & \sum_{j=1}^{N} Y(\mu_1, \ldots, \mu_{j-1}, X_j, \mu_{j+1}, \ldots, \mu_N) \\ & - (N-1)Y(\mu_1, \ldots, \mu_N) \end{aligned} \tag{4}$$

Using additive decomposition, the estimation of the statistical moments or uncertainty quantification of the system responses becomes much simpler. For the quality assessment of the assembly product, the statistical moments for the responses are considered in Eq. (5) as

$$\mathcal{E}[Y^m(\mathbf{X})] \cong \mathcal{E}\{Y_a^m\} = \int_{-\infty}^{\infty} Y_a^m \cdot f_{\mathbf{X}}(\mathbf{x}) \cdot d\mathbf{x}$$

where

$$Y_a = \sum_{j=1}^{N} Y(\mu_1, \ldots, \mu_{j-1}, X_j, \mu_{j+1}, \ldots, \mu_N) - (N-1) \cdot Y(\mu_1, \ldots, \mu_N) \tag{5}$$

Uncertainty of system responses can therefore be evaluated through multiple one-dimensional numerical integrations. The remaining challenge of the problem is how to carry out one-dimensional integration effectively. Using numerical integration, the one-dimensional integrations will be performed with integration weights $w_{j,i}$ and points $x_{j,i}$ using Eq. (6)

$$\begin{aligned} & \mathcal{E}\left[\sum_{j=1}^{N} Y^m(\mu_1, \ldots, \mu_{j-1}, X_j, \mu_{j+1}, \ldots, \mu_N)\right] \\ & \cong \sum_{j=1}^{N} \sum_{i=1}^{k-1} w_{j,i} Y^m(\mu_1, \ldots, \mu_{j-1}, x_{j,i}, \mu_{j+1}, \ldots, \mu_N) \end{aligned} \tag{6}$$

The number of integration points determines computational efficiency of the DR method. In general, the univariate DR method uses $kN+1$ integration points, where $N$ is the number of input random parameters and $k$ is the number of integration points along each axis excluding the sample at the mean. It is suggested that $k$ must be maintained at 2, or at most, 4, for large-scale engineering problems.

Using the DR method, three difficulties (inaccuracy, inefficiency, and singularity) are found while considering nonlinear applications. For highly nonlinear problems, the use of $2N+1$ or $4N+1$ integration points is not sufficient enough to capture the true nature of the problem. Inaccuracy can be resolved via increasing the number of integration points. However, this increases computational cost substantially. The DR method suggests the use of a moment based quadrature rule for the numerical integration. It requires only statistical information of the random input parameters and generates the integration points and weights for numerical integration. Unfortunately, the large amount of integration points to characterize a nonlinear problem requires high-order statistical moments of the input parameters to be known. It has been shown in Ref. [13] that the use of high-order statistical moments creates a singularity problem in determining the weights and integration points.

**4.2 Enhanced Dimension Reduction (EDR) Method.** The DR method is enhanced by incorporating a more robust one-dimensional numerical integration scheme. It is referred to as the eDR method [14]. Compared to the DR method, the eDR method increases the efficiency by using a stepwise moving least squares (SMLS) method. It generates approximate response values, $\hat{Y}(\mu_1, \ldots, \mu_{j-1}, x_{j,i}, \mu_{j+1}, \ldots, \mu_N)$, at all integration points along each random input in Eq. (7). Since a large number of integration points can be employed, the eDR method is more accurate than the DR method. This is possible since the SMLS method produces highly accurate one-dimensional responses. This approximate response allows the incorporation of any numerical integration method.

$$\begin{aligned} & \mathcal{E}\left[\sum_{j=1}^{N} Y^m(\mu_1, \ldots, \mu_{j-1}, X_j, \mu_{j+1}, \ldots, \mu_N)\right] \\ & \cong \sum_{j=1}^{N} \sum_{i=1}^{n} w_{j,i} Y^m(\mu_1, \ldots, \mu_{j-1}, x_{j,i}, \mu_{j+1}, \ldots, \mu_N) \\ & \cong \sum_{j=1}^{N} \sum_{i=1}^{n} w_{j,i} \hat{Y}^m(\mu_1, \ldots, \mu_{j-1}, x_{j,i}, \mu_{j+1}, \ldots, \mu_N) \end{aligned} \tag{7}$$

To recover singularity of the DR method due to a moment based quadrature rule, it is suggested in Ref. [14] that the eDR method use the adaptive Simpson rule as an alternative integration approach. This allows more flexibility for the eDR method to handle any distribution type encountered in practical engineering problems. Consequently, the eDR method turns out to be more efficient, accurate, and stable than the DR method.

The numerical procedure for the eDR method has the following steps:

1. Define a reasonable set of sample points to be used for the SMLS method, usually $2N+1$ or $4N+1$, depending on available resources and any prior knowledge of system nonlinearity. It is suggested that for a $2N+1$ sample size, $\mu$ and $\mu \pm 3\sigma$ will be used and for a $4N+1$ sample size it will also use $\mu \pm \sigma$. The determination of the sample size totally depends on the degree of nonlinearity in system performances [14]. If a performance is highly nonlinear, the $4N+1$ is used. Otherwise, $2N+1$ may be employed for the eDR method. However, if one parameter is known to be extremely nonlinear, additional sample points for that variable should be performed. It should be noted that this does not require additional samples along the remaining dimensions;
2. Perform one-dimensional function approximations for all random input parameters using the SMLS method;
3. Perform numerical integration using the adaptive Simpson rule to calculate statistical moments for all approximate functions in Eq. (5); and
4. Create probability density (or distribution) function based on statistical moments using a stabilized Pearson system [17,18].

## 5 Case Study

The proposed methodology is illustrated with an example representing the assembly of a hood-pin bracket. As seen in Fig. 2, the bracket consists of the attachment element and the locating pin for the hood. The location of the pin is a critical dimension that determines the appearance (gap and flushness) and closure effort of the hood. The material of each component is a mild steel with

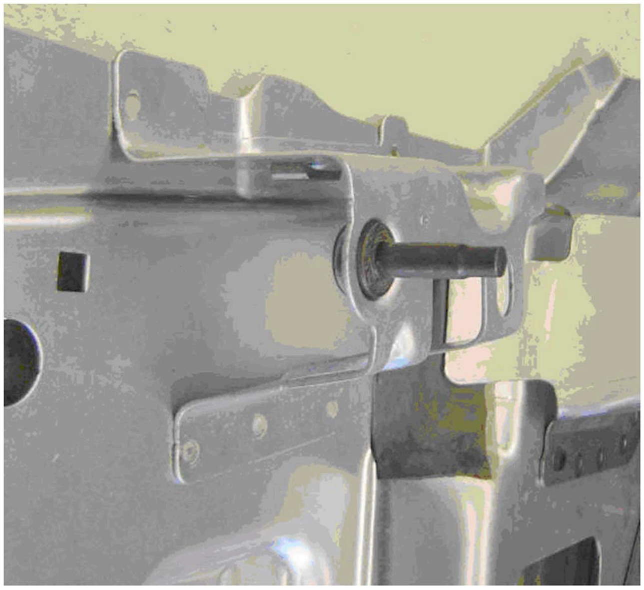

Fig. 2 Hood bracket

Young modulus $E=20{,}700\ \mathrm{N/mm^2}$ and Poison's ratio $\nu=0.3$. The approximate length and height of this assembly is 150 mm by 150 mm.

The ABAQUS model was developed to replicate the assembly process, as shown in Fig. 4. The assembly of the bracket includes two components: the bracket itself including the locating pin for the hood and the fender. Three contact areas have been identified for this assembly. Each contact area defines a set of contact element pairs between the two components. These contact areas 1, 2, and 3 are circled in Fig. 3. Two additional contact areas are identified in the model; these areas correspond to the contact between the welding tool and the components. These contact pairs (4 and 5) are indicated by rectangles in Fig. 3. The friction coefficient is assigned a value of 0.1. In order to improve the convergence of the model, a fine mesh is considered around the contact areas. The contact pairs are used to avoid the penetration between components and between a tool (clamp or welding gun) and the assembly components.

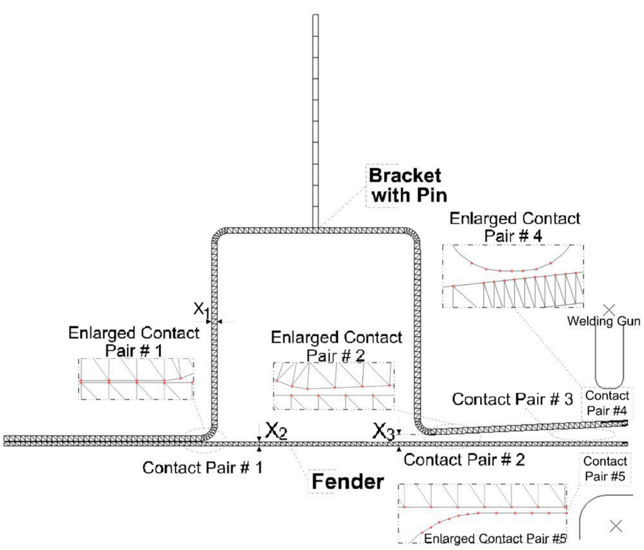


Fig. 3 Hood bracket assembly model

Table 2 Random input parameters

| Random variable | Physical property | Distribution | Mean (mm) | Range (mm) |
|---|---|---|---|---|
| $x_1$ | Thickness Component 1 | Beta | 1.1 | 0.9–1.3 |
| $x_2$ | Thickness Component 2 | Beta | 1.0 | 0.7–1.3 |
| $x_3$ | Corner gap | Beta | 1.5 | 0.0–3.0 |
| $x_4$ | Flange gap | Beta | 3.0 | 0.0–6.0 |

Four possible sources of variation have been simulated in the assembly. The sources of variation are represented as dimensional geometric errors in each component. As shown in Fig. 3, the sources of variation are: the material thickness of the bracket and fender, $x_1$ and $x_2$, respectively; the corner gap, $x_3$; and the flange gap, $x_4$. These dimensional errors are normally caused by the manufacturing process producing these two components. The FE model is parameterized to include these four variables, which are specified in Table 2. A beta distribution is used to describe the random behavior of the input variables to avoid outliers in the distributions that may cause difficulty in the convergence of the finite element model. The key product characteristics in the bracket assembly are the angle and location of the hood pin. The objective of the analysis is to determine the angle change on the pin after assembly. Simulations are conducted to determine the statistical distribution and parameters that describe the random nature of the angle after assembly due to the input variation on the variables $x_1, x_2, x_3$, and $x_4$.

The assembly process is simulated following the methodology presented in Fig. 1. First, the assembly components are located in the station using a set of locators. The displacement of the left flange on the bracket is constrained in all three DOFs ($t_x$, $t_y$, and $r_{xy}$ in the 2D plane model), where $t_x$, $t_y$, and $r_{xy}$ are the translational displacements along horizontal and vertical axes and the rotational displacement on the 2D plane, respectively. The fender is located using two locators at each extreme constraining the three DOFs. The assembly simulation begins approaching the lower electrode of the welding gun to the fender and moving the upper electrode downward in order to close the gap between the right ends of the two components. After the right end of the components has been deformed, the vertical distance between the welding gun tools is maintained at the combined thickness of the two parts (e.g., $x_1+x_2$). Then, both components are joined together using the bonded contact property and the connector elements in the welding area not allowing for any separation. Finally, the welding gun and the fixture at the right end of fender are removed, which results in the assembly springback. Figure 4 shows the change in the hood-pin angle before and after assembly. As can be seen in the figure, the angle of the pin does not recover its nominal position due to the assembly's new constraints.

**5.1 Results From the Noncontact Model and Contact Model.** In order to compare the results from the new contact assembly methodology with respect to the traditional linear noncontact assembly modeling, an MCS without considering contact between the components or tools was conducted. The difference of the effect between the noncontact model and contact model is showed graphically in Fig. 5. As shown in the figure, the main limitation of the linear assembly modeling is the penetration of the bracket into the fender. Figure 5(*a*) shows the expected results using traditional MIC. As can be seen, the components penetration remains after assembly. Even though this condition is physically impossible, these results are common in assembly modeling. The proposed methodology result for contact assemblies is presented in Fig. 5(*b*). Penetration between components is eliminated. This solution provides a closer estimation of the physical phenomenon.

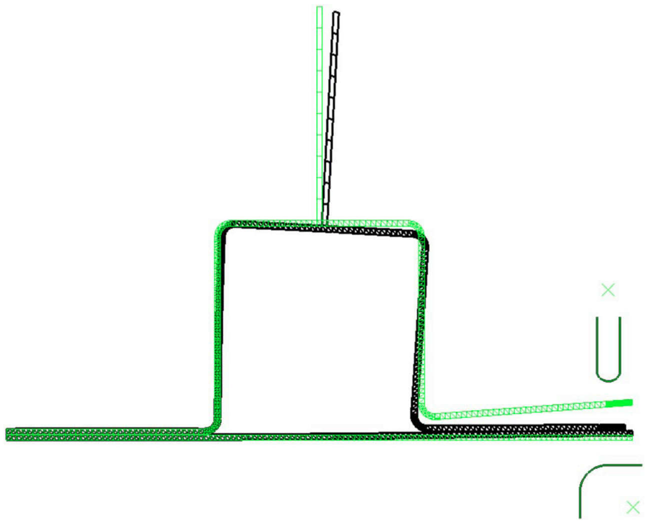

Fig. 4 Finite element results from before and after assembly

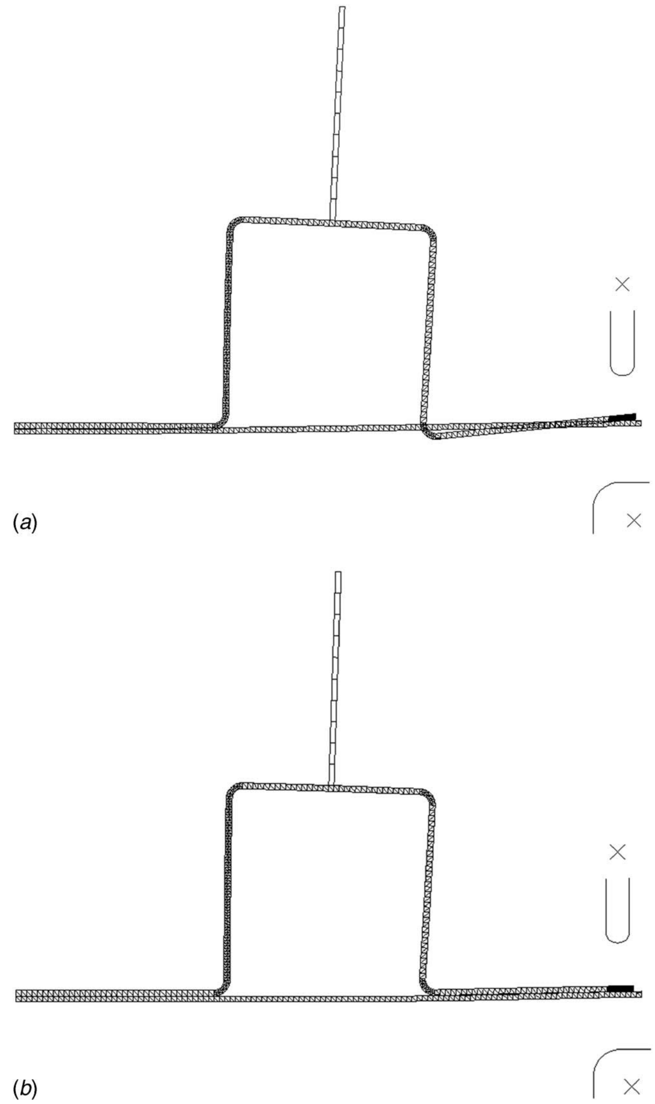

Fig. 5 Finite element results after assembly, noncontact, and contact linear models: (*a*) noncontact model; and (*b*) contact linear model

**5.2 Nonlinear Contact Modeling Results.** Using the predictive nonlinear contact assembly model, the assembly of the hood-bracket was studied. The relationship between the input variables $x_i$, shown in Table 2, and output variable $y$, the hood-pin angle, was studied. First, the nonlinearity of the assembly response was analyzed. After an initial analysis, the variables $x_3$ and $x_4$ were identified as being significant to the response nonlinearity. In other words, the pin angle is more sensitive to changes on the shape of the bracket (parameters $x_3$ and $x_4$) than to changes in the thicknesses of the components (parameters $x_1$ and $x_2$). The nonlinearity relation between the pin angle and the variables $x_3$ and $x_4$ was investigated by building a response surface with multiple simulation runs, as shown in Fig. 6. For this study, two cases were considered: compliant assemblies with and without contact considerations. In the case of the linear model without contact, 15 points equally distributed along each range of $x_3$ and $x_4$ were sampled, while keeping $x_1$ and $x_2$ at their mean values. The pin angle was determined for the 225 data points. Figure 6(*a*) shows the results for the noncontact model results. As can be seen, the angle of the pin is independent of the variable $x_3$. This can be explained because any change in the variable $x_4$ only increases the penetration between the components without affecting the spring-back of the assembly. In contrast, the response surface for the contact model was built with 20 equally spaced samples along the $x_3$ and $x_4$ range. Therefore, a total of 400 finite element runs were conducted to study the nonlinearity of the pin angle. Figure 6(*b*) shows the nonlinear relationship between the input variables $x_3$ and $x_4$ and the output variable $y$ for the contact model. Three zones can be identified in the figure. First, Zone 1 corresponds to the cases where the two components never become in contact, except for the welding area. Zone 2 corresponds to the cases where the two components experience a weak contact. Weak contact means that the contact is observed as the corner section of the upper component pushes the bottom component down; however no significant component deformation occurs. Finally, Zone 3 corresponds to the case when the components significantly deform during the assembly process due to the component interference. During this interaction the corner section of the upper component first pushes the bottom component down until it reaches the most deformation, and then the corner section of the upper component is forced to move to the left along the top surface of the bottom component to compensate for the deformation on the flange.

**5.3 Pin Angle Prediction Using EDR Method and Monte Carlo Simulation.** Direct MCS is performed by artificially generating a set of random numbers (5000 sample size) for variables $x_1$, $x_2$, $x_3$, and $x_4$. Those variables are assumed to follow an independent beta distribution with random properties in Table 2. A beta distribution is used to describe the random behavior of these variables to avoid outliers in the distributions that may cause difficulty in the convergence of the finite element model. The sample size is chosen based on the following criteria: accuracy and efficiency of the predictive model. The predicted model will be compared between the MCS and the eDR methods in terms of the PDF and statistical moments.

The flow chart for the enhanced dimensional reduction method combined with the predictive model for contact assembly is shown in Fig. 7. The eDR method used $4N+1$ sampling points to predict random behavior of the pin angle, where $N=4$, generating a total of 17 sample points, which are evaluated using the FE analysis. The sample points are chosen by the method discussed in Step 1 of the eDR methodology. These sample points are listed in Table 3. While employing the eDR method for uncertainty propagation of the pin angle, one-dimensional response approximation must be performed along each random variable using the SMLS method. To show the accuracy of the stepwise moving least square method, the response with respect to $x_4$ and 25 FE analyses, where $x_1$, $x_2$, and $x_3$ remain constant, is shown in Fig. 8. As can be seen

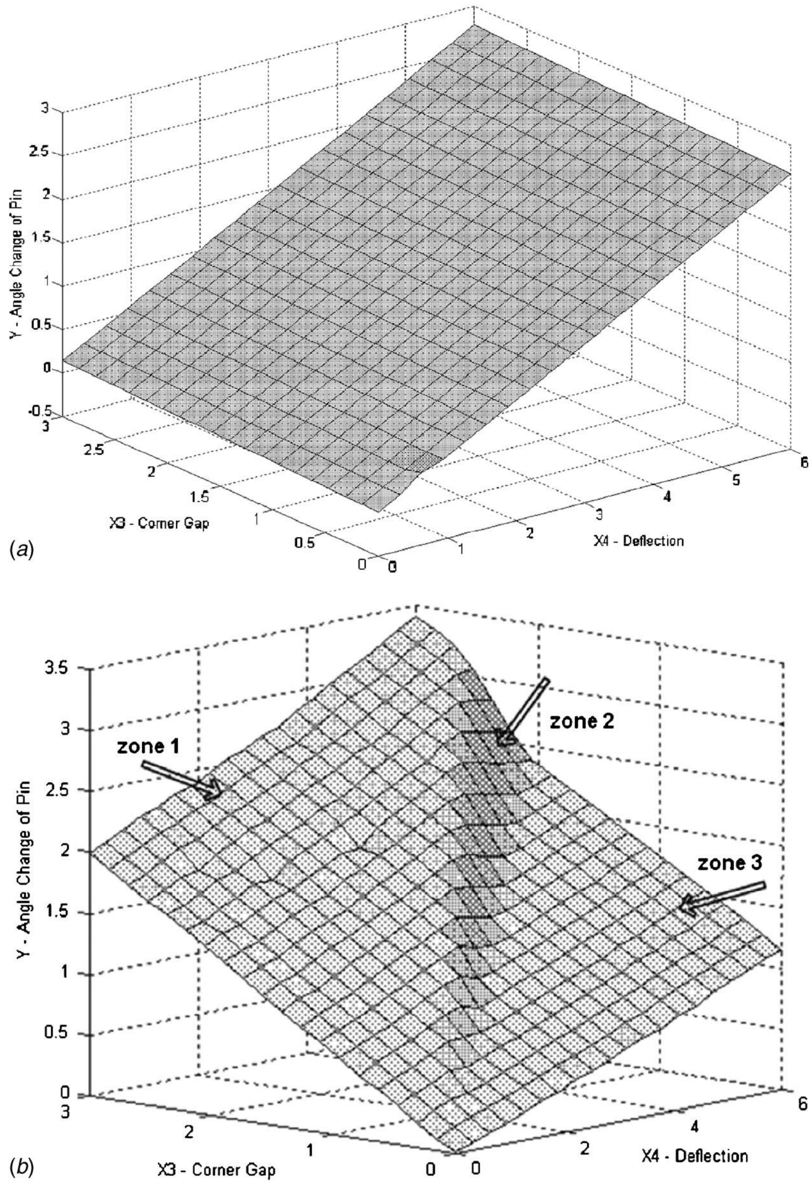


**Fig. 6 Angle response with respect to variables ×3 and ×4: (*a*) noncontact model; and (*b*) contact model**

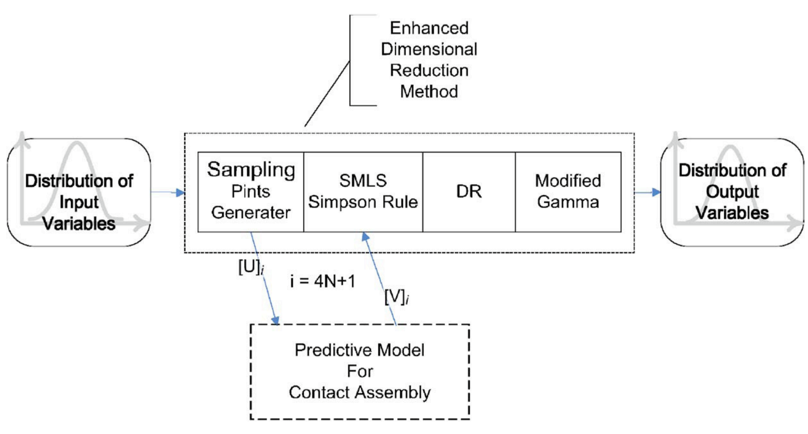


**Fig. 7 The eDR method with predictive contact model**

**Table 3 4$N$+1 sampling points and assembly response for the eDR method**

| $x_1$ | $x_2$ | $x_3$ | $x_4$ | $Y$ |
|---|---|---|---|---|
| 0.9 | 1 | 1.5 | 3 | 1.8054 |
| 1 | 1 | 1.5 | 3 | 1.7514 |
| 1.2 | 1 | 1.5 | 3 | 1.6357 |
| 1.3 | 1 | 1.5 | 3 | 1.582 |
| 1.1 | 0.7 | 1.5 | 3 | 1.4966 |
| 1.1 | 0.85 | 1.5 | 3 | 1.6002 |
| 1.1 | 1.15 | 1.5 | 3 | 1.7696 |
| 1.1 | 1.3 | 1.5 | 3 | 1.8276 |
| 1.1 | 1 | 0 | 3 | 0.54317 |
| 1.1 | 1 | 0.75 | 3 | 0.99872 |
| 1.1 | 1 | 2.25 | 3 | 2.2272 |
| 1.1 | 1 | 3 | 3 | 2.6692 |
| 1.1 | 1 | 1.5 | 3 | 1.6933 |
| 1.1 | 1 | 1.5 | 0 | 1.0414 |
| 1.1 | 1 | 1.5 | 1.5 | 1.3444 |
| 1.1 | 1 | 1.5 | 4.5 | 1.7431 |
| 1.1 | 1 | 1.5 | 6 | 2.0324 |

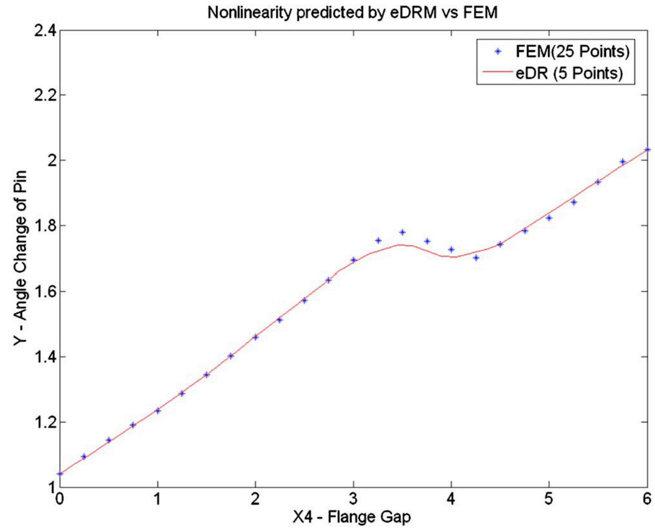


**Fig. 8 Nonlinearity prediction using stepwise moving least squares method**

the stepwise moving least squares method accurately approximates the response function. The response with respect to $x_4$ is the most nonlinear of the four input parameters, therefore all four responses can be accurately approximated with this method.

In addition, in order to compare the advantages of the proposed eDR method to model the nonlinear assembly processes, a traditional Taylor series expansion approach is used to estimate the statistical moments. The equations are shown in Table 4 where $\Delta x_i$ is considered as 0.5% of the range w.r.t. the corresponding $x_i$. The first-order Taylor series needs nine sample points and the second-order Taylor series needs 33 sample points (including the nine points required by first-order Taylor series). The statistical moments estimates obtained via Taylor series expansion are presented in Table 5. From these results, the second-order Taylor expansion predicts a larger error for the mean than eDR and even a linear first-order Taylor expansion. This discrepancy can be explained due to the nonlinear behavior of the assembly response. The nonlinear region of this model is away from the center of the response surface (Fig. 7($b$)) while the Taylor is expanded around the center point of the response surface. The larger error term of first-order Taylor expansion accidently made the mean closer to real.

As shown in Table 5, the eDR method estimated random behavior of the pin angle accurately and efficiently, compared to the MCS. This is also verified from the PDF approximation, as shown in Fig. 9. The compared results of noncontact and contact models are shown in Table 5. MCS was used for the noncontact model to predict the output distribution. For the contact model, MCS along with the eDR method were used to approximate the output uncertainty. The error percentage between the solutions of the MCS and the eDR method for the contact model is also shown in the table. The CPU time is the accumulated time starting from submitting the ABAQUS input file to the ABAQUS analysis solver until the

**Table 4 Statistical moments based on Taylor series expansion**

| | Taylor series expansion | Statistical moments |
|---|---|---|
| First-order Taylor expansion | $Y(X) \cong Y(\mu_X) + \sum_{i=1}^{4} \partial Y(\mu_X) / \partial x_i \Delta x_i$ | $\mu_Y \cong Y(\mu_X)$ <br> $\sigma_Y^2 \cong \sum_{i=1}^{4} \left(\partial Y(\mu_X) / \partial x_i\right)^2 \sigma_{x_i}^2$ |
| Second-order Taylor expansion | $Y(X) \cong Y(\mu_X) + \sum_{i=1}^{4} \partial Y(\mu_X) / \partial x_i \Delta x_i + \sum_{i=1}^{4} \sum_{j=1}^{4} \partial^2 Y(\mu_X) / \partial x_i \partial x_j \Delta x_i \Delta x_j$ | $\mu_Y \cong Y(\mu_X) + \frac{1}{2} \sum_{i=1}^{4} \partial^2 Y(\mu_X) / \partial x_i^2 \sigma_{x_i}^2$ <br> $\sigma_Y^2 \cong \sum_{i=1}^{4} \left(\partial Y(\mu_X) / \partial x_i\right)^2 \sigma_{x_i}^2 + \frac{1}{2} \sum_{i=1}^{4} \sum_{j=1}^{4} \partial^2 Y(\mu_X) / \partial x_i \partial x_j \sigma_{x_i}^2 \sigma_{x_j}^2$ |

**Table 5 Moments estimation results**

| Model | No contact | With contact | | | |
|---|---|---|---|---|---|
| Method | MCS | MCS | eDRM (error) | First-order Taylor expansion (error) | Second-order Taylor expansion (error) |
| Mean(mm) | 1.3653 | 1.6028 | 1.5811 (1.35%) | 1.6165 (0.85%) | 1.4125 (11.87%) |
| Std. dev. | 0.4577 | 0.4423 | 0.4402 (0.48%) | 0.4621 (4.47%) | 0.4621 (4.47%) |
| No of FEAs | 5,000 | 5,000 | 17 | 9 | 33 |
| CPU time (min) | 7,500 | 10,000 | 34 | 18 | 66 |

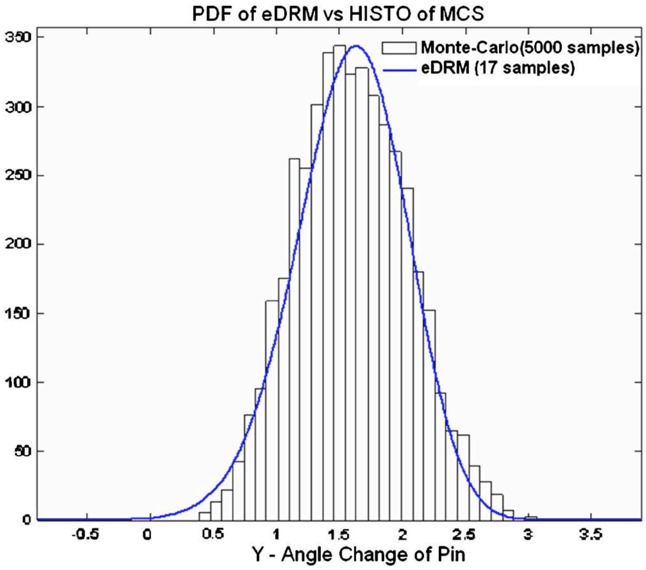


**Fig. 9 MCS histogram and eDR method PDF**

ABAQUS solver finishes the simulation. It is evident that the eDR shows good agreement in the mean and standard deviation with the MCS. As shown in Fig. 6 that the pin angle response must hold highly nonlinear interactions between $x_3$ and $x_4$, since the stepwise response runs along the diagonal direction of $x_3$ and $x_4$. According to the error analysis of the eDR method, numerical error can be accumulated from biquadratic terms or higher. It is thus obvious that numerical error is mainly due to highly nonlinear interaction between $x_3$ and $x_4$. It is also expected that the MCS will yield a minor degree of the error due to a finite number of samples.

As shown in Fig. 9, there is a good correlation between the histogram from the MCS and the PDF from the eDR method. So, this case study shows that the eDR method produces an excellent estimate of the uncertainty propagation of the highly nonlinear assembly process.

## 6 Conclusions

This paper presents a new methodology for variation propagation modeling on compliant assemblies that include the contact effect between components and assembly tools (fixtures and welding tools). The methodology is based on finite element methods. A parametric model is used in order to incorporate the input variation from different variables. In addition, several elements to improve finite element convergence were implemented. The new model response from contact assembly is nonlinear; therefore, the traditional sensitivity analysis is not adequate to estimate the statistical response of the characteristics of the assembly. In order to improve the efficiency of the methodology compared with MCS methods, the eDR method is used to sample and estimate the statistical response of the system. A case study is presented for the assembly of an automotive hood bracket. The proposed methodology combined with eDR produces an excellent estimate of the uncertainty propagation on highly nonlinear assembly processes.

## References


[1] Ding, Y., Ceglarek, D., and Shi, J., 2000, "Modeling and Diagnosis of Multistage Manufacturing Process: Part I—State Space Model," *Proceedings Japan–USA Symposium of Flexible Automation*, Ann Arbor, MI, July 23–26.

[2] Mantripragada, R., and Whitney, D. E., 1999, "Modeling and Controlling Variation Propagation in Mechanical Assemblies Using State Transition Models," IEEE Trans. Rob. Autom., **115**(1), pp. 124–140.

[3] Liu, S. C., and Hu, S. J., 1997, "Variation Simulation for Deformable Sheet Metal Assemblies Using Finite Element Methods," ASME J. Manuf. Sci. Eng., **119**, pp. 368–374.

[4] Camelio, J., Hu, S. J., and Ceglarek, D., 2003, "Modeling Variation Propagation of Multi-Station Assembly Systems With Compliant Parts," ASME J. Mech. Des., **125**(4), pp. 673–681.

[5] Camelio, J., and Hu, S. J., 2004, "Compliant Assembly Variation Analysis Using Components Geometric Covariance," ASME J. Manuf. Sci. Eng., **126**(2), pp. 355–360.

[6] Dahlstrom, S., and Lindkvist, L., 2006, "Variation Simulation of Sheet Metal Assemblies Using the Method of Influence Coefficients With Contact Modeling," Ph.D. thesis, Chalmers University of Technology, Gothenburg, Sweden.

[7] Cai, W., Hsieh, C., Long, Y., Martin, S., and Oh, K., 2006, "Digital Panel Assembly Methodologies and Applications for Compliant Sheet Components," ASME J. Manuf. Sci. Eng., **128**(1), pp. 270–279.

[8] Myers, H. R., and Montgomery, D. C., 1995, *Response Surface Methodology*, Wiley, New York, NY.

[9] Youn, B. D., Choi, K. K., Gu, L., and Yang, R. J., 2004, "Reliability-Based Design Optimization for Crashworthiness of Side Impact," Struct. Multidiscip. Optim., **26**(3–4), pp. 272–283.

[10] Wu, W.-T., Griffin, J. H., and Wickert, J. A., 1995, "Perturbation Method for the Floquet Eigenvalues and Stability Boundary of Periodic Linear Systems," J. Sound Vib., **182**(2), pp. 245–257.

[11] Alefeld, G., and Herzberger, J., 1983, *Introduction to Interval Computations*, Academic, New York, NY.

[12] Halder, A., and Mahadevan, S., 2000, *Probability, Reliability, and Statistical Methods in Engineering Design*, Wiley, New York, NY.

[13] Xu, H., and Rahman, S., 2004, "A Generalized Dimension-Reduction Method for Multi-dimensional Integration in Stochastic Mechanics," Int. J. Numer. Methods Eng., **61**, pp. 1992–2019.

[14] Youn, B. D., Zhimin, X., Wells, L. J., and Lamb, D. A., 2006, "The Enhanced Dimension-Reduction (eDR) Method for Reliability-Based Robust Design Optimization," *Proceedings AIAA-MAO 2006-6977*, Portsmouth, VA, Sept. 6–8.

[15] Chase, K. W., and Parkinson, A. R., 1991, "A Survey of Research in the Application of Tolerance Analysis to the Design of Mechanical Assemblies," Res. Eng. Des., **3**, pp. 23–37.

[16] Rahman, S., and Xu, H., 2004, "A Univariate Dimension-Reduction Method for Multi-Dimensional Integration in Stochastic Mechanics," Probab. Eng. Mech., **19**, pp. 393–408.

[17] Youn, B. D., Xi, Z., Wells, L. J., and Lamb, D. A., 2006, "Stochastic Response Surface Using the Enhanced Dimension-Reduction (eDR) Method for Reliability-Based Robust Design Optimization," *Proceedings 11th AIAA/ISSMO MAO Conference*, Portsmouth, VA, Sept. 6–8.

[18] Johnson, N. L., Kotz, S., and Balakrishnan, N., 1994, *Continuous Univariate Distributions*, Wiley-Interscience, New York, NY.